

STRONG GROUND MOTION SIMULATION OF THE JANUARY 13, 2001 EL SALVADOR EARTHQUAKE USING EMPIRICAL GREEN'S FUNCTION METHOD

Nelson Eduardo Ayala Leiva*
MEE08157

Supervisor: Toshiaki YOKOI**

ABSTRACT

In January and February 2001, a very intense seismic activity occurred in El Salvador, it caused many damages in the country. The biggest two earthquakes with magnitude $M_w=7.7$ and $M_w=6.5$ occurred exactly one month separation, the first one occurred on January 13 and the second one on February 13.

Using the empirical Green's function method we simulated the January 13, 2001 earthquake using strong ground motion data (accelerograms) and an aftershock with magnitude $M_w=5.7$. We used source spectral fitting method in order to find an estimation of parameters to be used in EGF method.

Two fault plane models determined by previous studies were considered for the simulation in this study. One has strike/ dip/ rake angles $306.^{\circ}/ 48.^{\circ}/ -107.^{\circ}$ and another $297.^{\circ}/ 58.^{\circ}/ -93.^{\circ}$, respectively. For the former we tested two possibilities with the same asperity area (30 km x 30 km) but different number of subfaults.

We performed the ground motion simulation for three stations with large PGA and PGV values and a clear directivity pulse. From the result we determined that the former fault model provided us with the best results obtained in this study. This fault model is composed by a grid of 36 subfaults with individual area of 5 km x 5 km.

Keywords: 2001 El Salvador earthquakes, Empirical Green's Function method, Strong Motion Records.

1. INTRODUCTION

El Salvador is a small country with 21,040 km² area and it is located in the Central America isthmus. The population is about 6 millions and is highly concentrated in the capital city, San Salvador, where about 1.8 millions are living now. The recent earthquakes on January 13 and February 13, 2001 showed the vulnerability of El Salvador. These earthquakes have affected not only the poorest people but also the middle-upper class. Many people were buried in landslides areas, other lost their houses and their relatives and many cities were not communicated because landslides obstructed the ways.

The seismicity of El Salvador is produced by three sources, the tectonics, the active fault system and the volcanic chain. The tectonics of Central America and Caribbean is composed of the interaction of five plates, The North American, Cocos, Caribbean, Nazca and South America plate. El Salvador is strongly affected by earthquakes generated in the zone where Cocos plate is subducting beneath the North American and Caribbean plates. The last strong and destructive event generated by this source occurred in January 13, 2001. The active fault system produces earthquakes with magnitude lower than 6.5, but they are too destructive due to the shallow focal depth. On February 13, 2001 occurred the last large event produced by this source.

*Universidad Centroamericana José Simeón Cañas.

** International Institute of Seismology and Earthquake Engineering, Building Research Institute, Japan.

2. METHODOLOGY.

In this study, a useful approach was applied to estimate strong ground motion for a large earthquake using the record of small earthquakes, considered as Empirical Green's Function, EGF, (Hartzell, 1978; Irikura, 1986; Irikura and Kamae, 1994) , being the main idea of the EGF method that small event has already included the properties of the propagation path and local site effects, so it is necessary to know the details of the velocity structure (Poiata, 2005). EGF takes in consideration two similarity relations between large and small events which are scaling relation of source parameters and scaling of source spectra.

In the first scaling relation, the parameters studied by Kanamori and Anderson (1975) and by Yokoi and Irikura (1991) are expressed by the following equation:

$$L/l = W/w = (M_o / m_o)^{1/3} = (C N^3)^{1/3}, \quad D/d = (C N^3)^{1/3}, \quad C = \Delta\sigma_L / \Delta\sigma_s \quad (1)$$

where L, l, W, w, M_o, m_o, D and d are fault lengths, fault widths, seismic moments and slip duration times for large and small event respectively. C is the stress drop correction factor and is defined as the ratio of stress drop for large event ($\Delta\sigma_L$) and small event ($\Delta\sigma_s$).

The second relation is represented by ω^{-2} source spectra scaling model (Aki, 1967) and (Brune, 1970). The shape of the source model is given by Eq. (2). In Eq. (2) f_c , f and U_o are spectral corner frequency, the low frequency, and flat level of displacement spectrum respectively, also f_c is proportional to the inverse of square root of the fault dimension $(LW)^{-1/2}$ and U_o is proportional to the seismic moment M_o .

$$U(f) = U_o / \{1 + (f/f_c)^2\}. \quad (2)$$

The second relation was studied by Aki (1967) and Brune (1970), and then it was modified by Irikura and Kamae (1994) by adding the stress drop correction factor. This relation is expressed by Eq. (3) and Eq. (4)

$$\frac{U_o}{u_o} = \frac{M_o}{m_o} = C N^3, \quad (3)$$

$$\frac{A_o}{a_o} = \left(\frac{M_o}{m_o} \right)^{1/3} = C N, \quad (4)$$

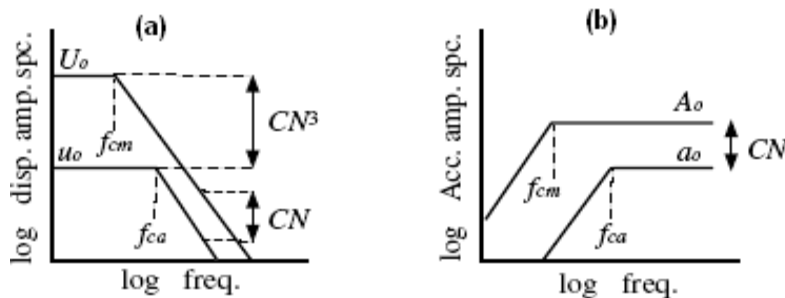


Fig. 1. a) Displacement source spectra. b) Acceleration source spectra (Poiata, 2005)

where U_o, u_o, A_o and a_o are flat level of displacement spectrum and flat level of acceleration spectrum for large and small events (Figure 1). To perform the simulation of strong ground motion it is necessary to find the values of N and C , then divide the fault plane in $N \times N$ sub faults as Fig. 2 shows.

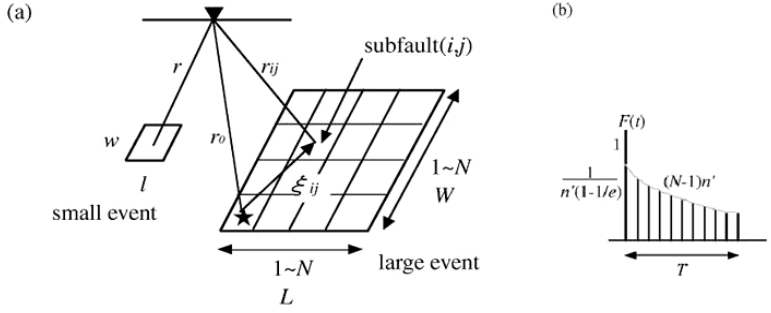


Figure 2. a) Schematic of fault parameters used for EGF.
b) Filtering function (Poiata, 2005)

The waveform of the target event $U(t)$ can be expressed in terms of the small event through Eq. (5) where t_{ij} and $F(t)$ have to be determined by equations (6) (Irikura et al, 1997).

$$U(t) = C \sum_{i=1}^N \sum_{j=1}^N \frac{r}{r_{ij}} F(t - t_{ij}) * u(t), \quad (5)$$

$$t_{ij} = \frac{r_{ij} - r_o}{\beta} + \frac{\xi_{ij}}{V_R}, \quad F(t) = \delta(t) + \frac{1}{n^{\left(1 - \frac{1}{e}\right)}} \sum_{k=1}^{(N-1)n'} \left\{ \frac{1}{(k-1)} \delta \left[t - t_{ij} - \frac{(k-1)T}{(N-1)n'} \right] \right\} \quad (6)$$

Here: r, r_{ij}, r_o are the respective distances from site to the hypocenter of small event, to (i, j) subfault and to starting point of rupture on the fault plane of large event; ξ_{ij} , distance between starting point and (i, j) subfault; β , shear wave velocity; V_R , rupture velocity; $F(t)$, filtering function; T , rise time of target event and n' , appropriate integer to eliminate spurious periodicity

3. DATA.

To perform this study we have used strong ground motion records from “Universidad Centroamericana José Simeón Cañas” (UCA University) network for events required in empirical Green’s function method (Figure 3). The UCA network by the time of the earthquake was constituted by 10 digital accelerographs type SSA-2 (Kinematics) located in the central area of the country as shown in Figure 3. A wider description of this strong motion network is presented by Boomer et al.

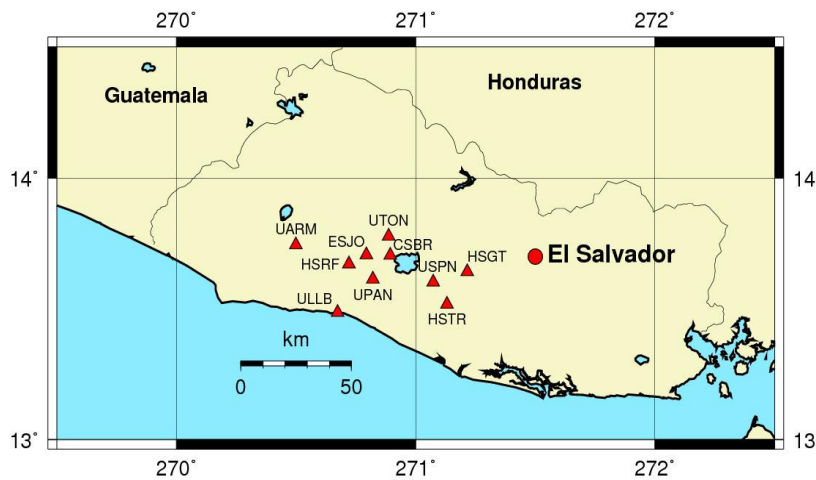


Figure 3. Distribution of stations of UCA strong ground motion network (triangles)

(1997). UCA strong ground motion network recorded the January 13, 2001 earthquake and 78 aftershocks. The main event was recorded at 9 stations. In the selection of the aftershock to be used as a small event in EGF method we selected the event recorded in the majority of the stations and with epicenter location near that of the main shock. To achieve this purpose we found the available information in USGS web site.

In order to achieve the purpose of this study we have taken into account two studies related with source characterization, we have considered their results as input in this study. The studies are:

- “The 13 January 2001 El Salvador earthquake: A multidata analysis”, (Vallée et al., 2003).
- “The January 13, 2001 Off the coast of El Salvador Earthquake, chapter 1, Source Characteristics and Strong Ground Motion”. (Pulido, 2001).

4. ANALYSIS.

Using the records of the main event and the selected aftershock we made a spectral analysis in order to determine the corner frequencies for both events. Figure 4 a) shows the acceleration spectra for 9 stations and it is possible to notice that the main event does not follow properly the ω^2 model, because of the decay rate at the lower frequency side. These spectra are smoothed using a Parzen window of the band width 0.30. The spectral ratios of the main shock events to the selected aftershock are calculated in order to cancel out the site and the path effect. The average of spectral ratio was calculated in order to correct the effect of radiation pattern, but also with the aim of preventing the involvement of possible non-linear effects in the spectral ratio’s average, we did not use the stations which recorded PGA’s values higher than 500 gals during the mainshock, Figure 4 b). We have used the available frequency range from 0.4 Hz to 4 Hz, the minimum is set in order to avoid the deviation due to noise included in the aftershock records for frequencies lower than 0.4 Hz, while the maximum is set at 4 Hz because of the decay of spectra in high frequency range due to the difference of f_{max} . We used the theoretical source spectral ratio fitting method proposed by Miyake et al. (1999) in order to find the corner frequency for the main event and the selected aftershock, namely f_{cm} and f_{ca} and the seismic moment ratio. Then it was necessary to fit the curve define by source spectral ratio function (SSRF). We set the frequency range for theoretical curve at the same values of the available frequency range explained above. The fitted curve and spectral ratio’s average are shown in Figure 4 c).

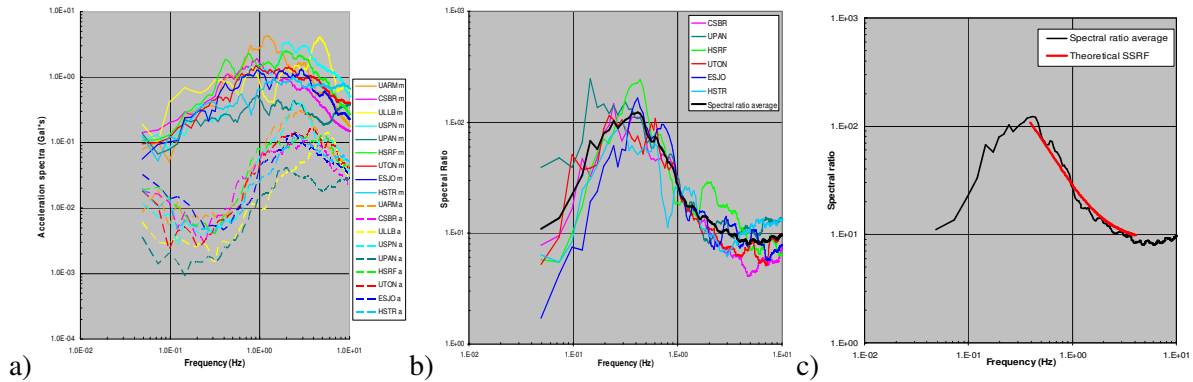


Figure 4. Spectral analysis. a) acceleration spectra, b) spectral ratio for stations with PGA’s lower than 500 gal. c) spectral ratio average and theoretical SSRF curve.

It is possible to find many values of M_o/m_o , f_{cm} and f_{ca} in the fitting of the theoretical curve, we found two sets that are showed in Table 1, that is deviated from the average seismic moment – corner frequency relation. Namely it is higher than the general trend according to its magnitude. It is, however, possible considering that intraslab earthquakes can have a high stress drop. We performed the simulation for three stations with high PGA values and with a clear directivity pulse. Using Case A values from Table 1 and the characteristics of faults and main asperity found by studies considered we started finding for good spectra and waveforms fitting using empirical Green’s function program. First we started using the fault plane model obtained by Pulido (2001). In the fitting of Vallée et al. (2003) fault model we conserved the subfault size but we modified N and C values.

Table 1. Values obtained from spectral ratio

Case	M_o/m_o	f_{cm} (Hz)	f_{ca} (Hz)	C	N
A	550	0.2	1.6	1.07	8
B	350	0.25	1.6	1.33	6

From the results obtained for cases mentioned before we determined that Pulido (2001) fault model gives a better approximation of synthetic waveforms and spectra than Vallée et al. (2003) fault model. Taking these results into account we performed the case B of spectral ratio fitting for Pulido (2001) fault model. A resume of all parameters for different cases is shown in Table 2. The results obtained for Pulido (2001) fault model using values for case B are shown in Figures 5 to 7.

Table 2. Parameters used for simulation in both fault models.

Parameters	Pulido et al (2001)		Vallée et al
	Case A	Case B	2003
Strike, Dip and Rake of main event (°)	306, 48, -107	306, 48, -107	297, 58, -93
Strike, Dip and Rake of aftershock (°)	303, 80, 147	303, 80, 147	303, 80, 147
Moment magnitude of main event/aftershock	7.6/5.7	7.6/5.7	7.7/5.7
Depth main/aftershock (km)	39.0/59.3	39.0/59.3	54.0/59.3
Rupture area (km ²)	70 x 70	70 x 70	70 x 70
Asperity area (along strike x along dip) (km)	30 x 30	30 x 30	50 x 25
Rupture/S-wave velocities (km/s)	2.9/3.99	2.9/3.99	3.5/4.4
Subfault area (dx and dw) (km)	3.75 x 3.75	5 x 5	3.75 x 3.75
dx0 and dw0 (km)	0, -2.50	0, 0	8.50, 7.50
nx, nw, nsx, nsy, c factor	8, 8, 1, 3, 2.5	6, 6, 1, 2, 3.2	13, 7, 4, 7, 2.0
Number of subfaults	64	36	91

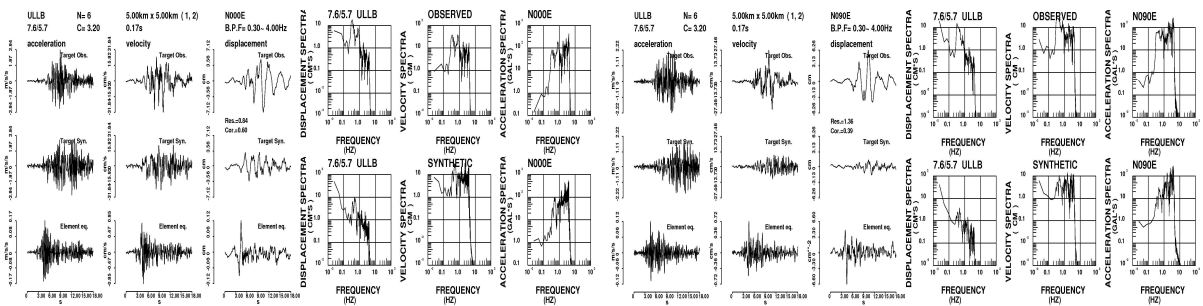


Figure 5. Waveform simulation for ULLB station using Pulido (2001) case B fault model, for N-S (two figures at left) and E-W (two figures at right) components.

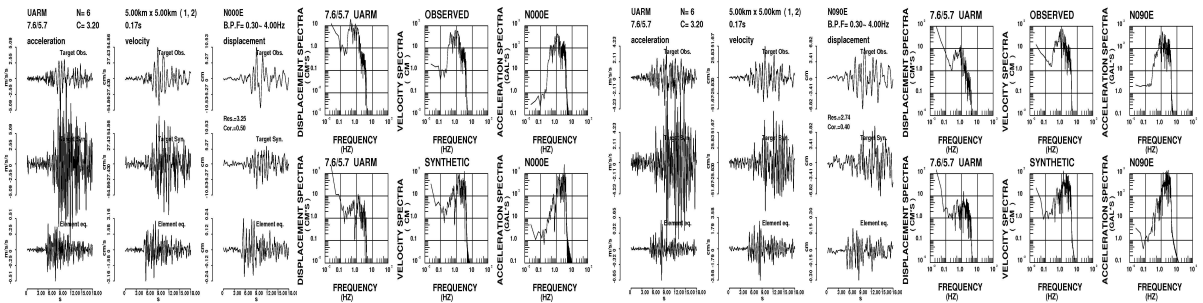


Figure 6. Waveform simulation for UARM station using Pulido (2001) case B fault model, for N-S (two figures at left) and E-W (two figures at right) components.

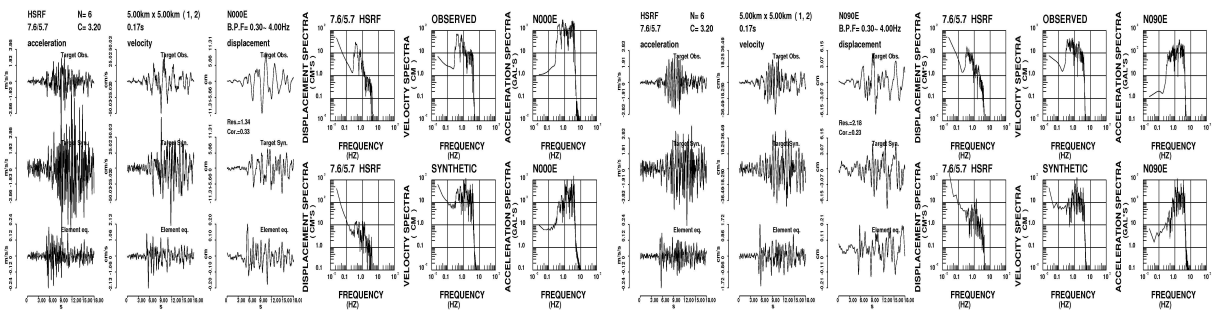


Figure 7. Waveform simulation for HSRF station using Pulido (2001) case B fault model, for N-S (two figures at left) and E-W (two figures at right) components.

5. CONCLUSIONS

Determination of the parameters for waveform synthesis is conducted using source spectral ration function (SSRF). All existing strong motion records are used to average out the radiation coefficient except those which have PGA bigger than 500 gals in order to prevent the non-linear effect. Fitting the theoretical curve defined by SSRF we found two possible sets for moment ratio - corner frequency pairs. For both of them the small event's corner frequency value is determined 1.6 Hz.

Two fault plane models determined by Pulido (2001) and Vallée et al. (2003) have been considered for the simulation in this study. Looking at the results obtained, Pulido (2001) fault model gives a better approximation between synthetic and observed spectra and waveforms of the selected three stations where a clear directivity pulse are observed. Considering two cases for Pulido (2001) fault model, the difference was not significant between case A and B in similarity between synthetic and observed waveforms and spectra related, but if we consider seismic moment values as 4.57×10^{27} dyne-cm and 3.81×10^{24} dyne-cm (Harvard-CMT) for main and small event respectively and Eq. (3) we find that synthetic events produce asperity seismic moments equivalent to 107% of total seismic moment of main event for case A. For case B it is only 57%. Taking into account both aspects mentioned above we select the Pulido (2001) case B fault model which provided the best results obtained in this study.

We determined that signal/noise ratio is not enough to reproduce well fitted synthetic displacement waveform and the low frequency part of acceleration, velocity and displacement synthetic spectra. This problem could be generated by ambient noise due the conditions in stations.

6. RECOMMENDATION

It is necessary to continue improving the study of fault characterization of the complexity of subducting zone and its earthquakes generated. It is essential to start studying the fault characterization of earthquakes produced by intraplate fault system and the volcanic chain. The study of the complex relationship between subduction source and intraplate fault system become necessary.

ACKNOWLEDGEMENT

I am very grateful with Dr. H. Miyake because this study was conducted using the program that she opens to public in internet. I thanks to UCA for provide me the strong motion data.

REFERENCES

- Aki, K., 1967, J. Geophys. Res., 72, 1217-1231.
Boomer, J. et al., 1997, Seismological Research Letters, vol. 68, N. 3, 426 – 437.
Brune, J. N., 1970, J. Geophys. Res. 75, 4997-5009.
ERI (Earthquake Research Institute), Hiroe Miyake. <http://www.eri.u-tokyo.ac.jp/hiroe/egfm/>
Hartzell, S. H., 1978, Geophysical Research letters, 5, 1-4.
Irikura, K., 1986, Proc. 7th Japan Earthq. Eng. Symp., 151-156.
Irikura, K. and Kamae, K., 1994, Annali di Geofisica, XXXVII, 25-47.
Irikura, K., Kagawa, T. and Sekigushi, H., 1997, Seism. Soc. Japan, 2, B25. (in Japanese).
Kanamori, H. and Anderson, D. L., 1975, Bull. Seismol. Soc. Am., 65, 1073-1095.
Miyake, H., Iwata, T. and Irikura, K., 1999, Zisin, Ser. 2, 51, 431-442 (in Japanese).
Poiata, N., 2005, Individual studies by participant at the IISEE, 41, 131-144.
Pulido, N. E. (2001), Japan Society of Civil Engineering.
Universidad Centroamericana (UCA), 2001, Strong motion data of January earthquakes in El Salvador
Vallée, M. and Bouchon M., 2003, Journal of Geophysical Res., vol. 108, N° B4, 2203, 7-1 to 7-19.
Yokoi, T and Irikura, K., 1991, Zisin, Ser. 2, 44, 109-122 (in Japanese).